Electronic Supporting Information

Reversible and efficient SO$_2$ capture by a chemically stable MOF CAU-10: Experiments and simulations

J. Antonio Zárate,[a,†] Eduardo Domínguez-Ojeda,[b,†] Elí Sánchez-González,[c] Eva Martínez-Ahumada,[a] Valeria B. López-Cervantes,[a] Daryl R. Williams,[d] Vladimir Martis,[e] Ilich A. Ibarra[*,a] and José Alejandre[*,b]

[a.] Laboratorio de Fisicoquímica y Reactividad de Superficies (LaFReS), Instituto de Investigaciones en Materiales, Universidad Nacional Autónoma de México, Circuito Exterior s/n, CU, Coyoacán, 04510, Ciudad de México, Mexico. E-mail: argel@unam.mx.

[b.] Departamento de Química, Universidad Autónoma Metropolitana-Iztapalapa, San Rafael Atlixco 186, Col. Vicentina, Iztapalapa, C. P. 09340 Ciudad de México, Mexico. E-mail: jra@xanum.uam.mx

[c.] Institute for Integrated Cell-Material Sciences (WPI-iCeMS), Kyoto University, Yoshida, Sakyo-ku, Kyoto 606-8501, Japan.

[d.] Surfaces and Particle Engineering Laboratory (SPEL), Department of Chemical Engineering, Imperial College London, South Kensington Campus, London SW7 2AZ, UK.

[e.] Surface Measurement Systems, Unit 5, Wharfside, Rosemont Road, London HA0 4PE, UK.

Experimental Section

Synthesis. The aluminum nitrate (1.35 g, 3.6 mmol) and the 1-3-benzenedicarboxylic acid (0.6 g, 3.6 mmol) were dissolved in a H_2O:DMF mixture (4:1, 12 cm³:3 cm³). Synthesis was carried out in a Teflon-lined autoclave (90 cm³) at 408 K for 12 h.[1]
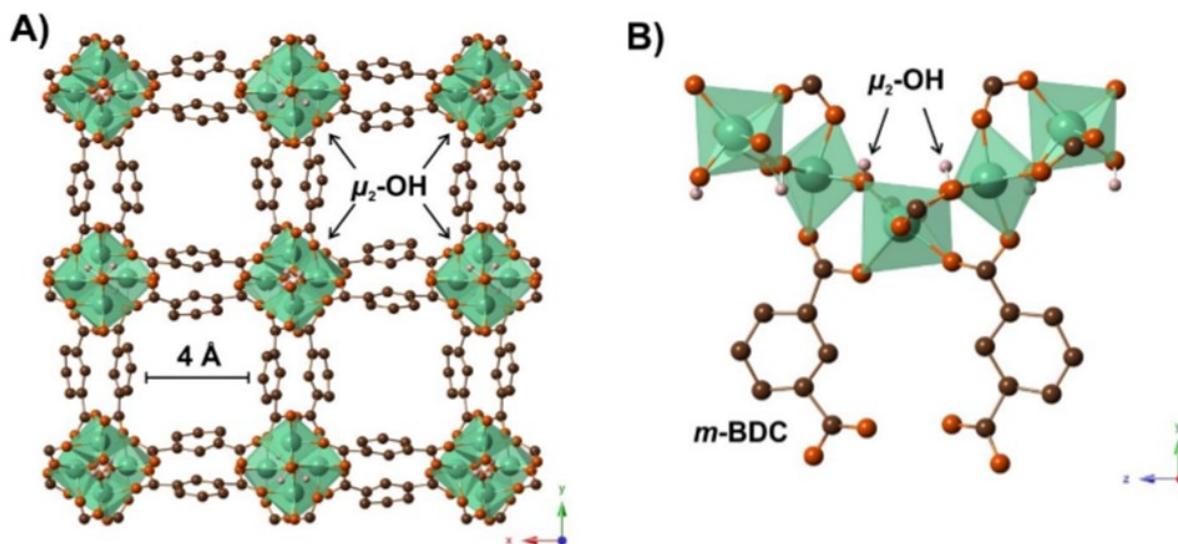

Fig. S1. Crystalline structure of CAU-10: A) view of one-dimensional channels through *c* axis; B) view of AlO6 octahedra interconnected by *m*-BDC ligands through *b* axis. (Reprinted with permission from ref. 1. Copyright 2018, Elsevier).

The PXRD pattern of the as-synthesised sample showed a good match with the simulated pattern (see Fig. S2).
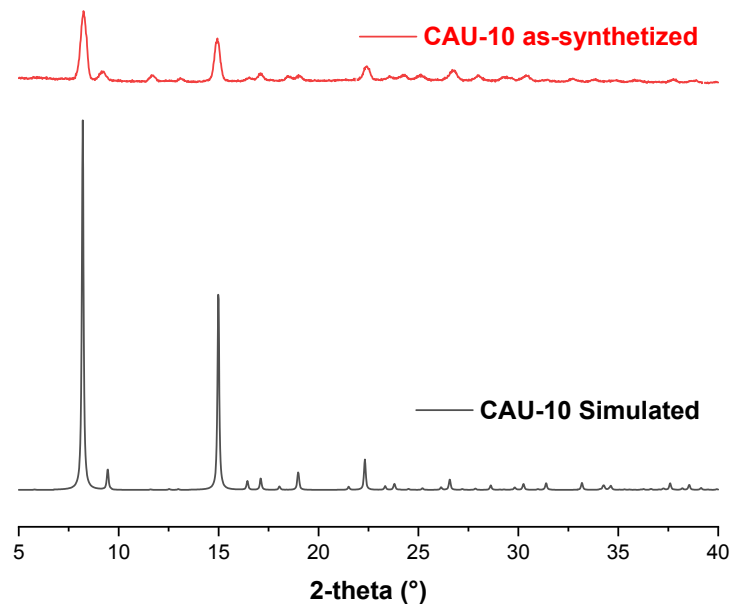
Fig. S2. Comparison of CAU-10 as-synthetized and simulated PXRD (λ = 1.5406 Å).

Adsorption isotherms of N_2 and SO_2

Prior measurements, the acetone-exchanged sample was activated at 423 K under dynamic vacuum ($1 \cdot 10^{-6}$ bar) for 70 min. SO_2 adsorption was carried out at 298 K up to 1 bar in a Dynamic Gravimetric Gas/Vapour Sorption Analyser, DVS vacuum (Surface Measurement Systems Ltd).
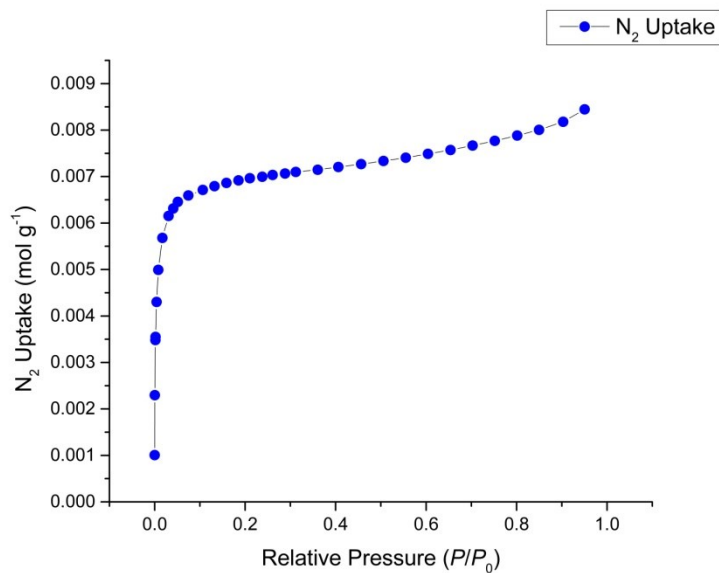

Fig. S3. N_2 adsorption isotherm at 77 K of as-synthesized CAU-10 material.

SO$_2$ adsorption exhibits a type-I isotherm (Fig. S4) with a maximum uptake of 4.47 mmol g^{-1} at 1 bar. The SO$_2$ adsorption capacity is lower than the reported for other Al-based MOFs (Table S1).
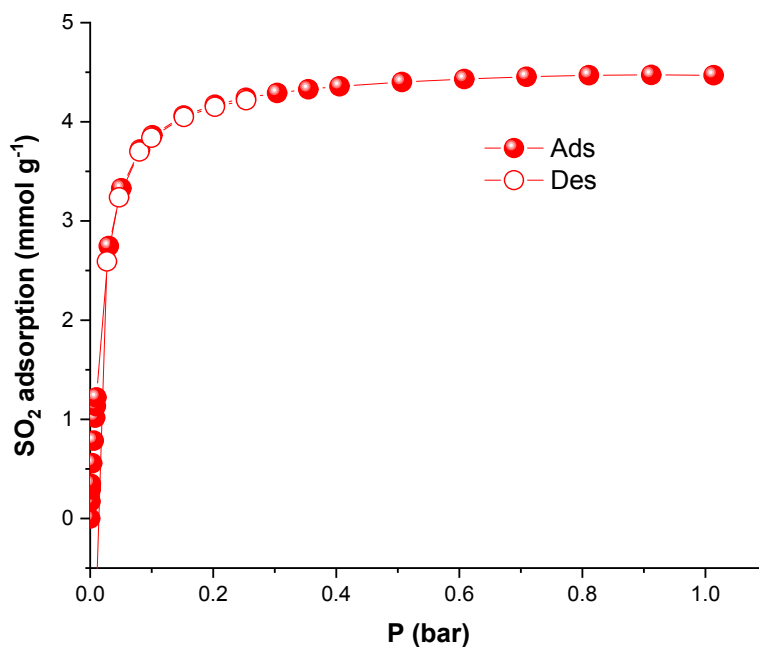

Fig. S4. CAU-10 SO$_2$ adsorption-desorption isotherms at 298 K.
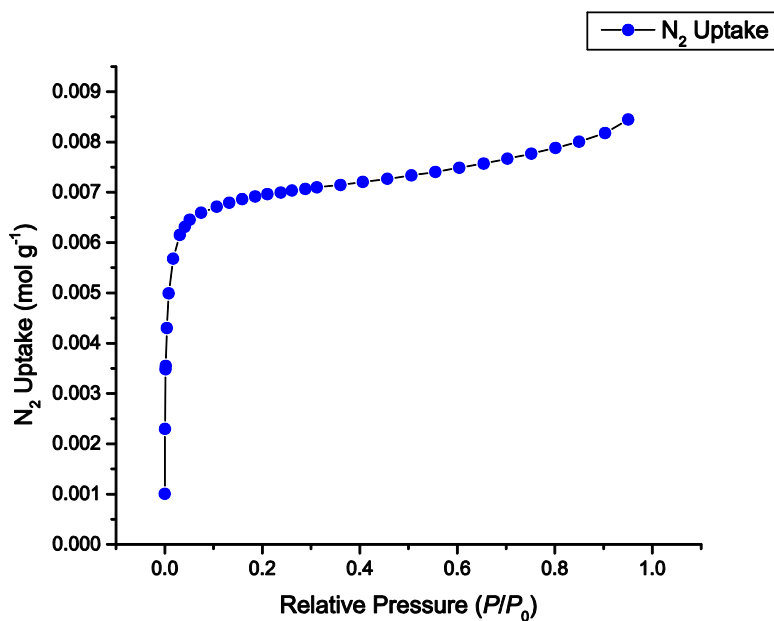

Fig. S5. N$_2$ adsorption isotherm at 77 K of CAU-10 after SO$_2$ adsorption experiment.
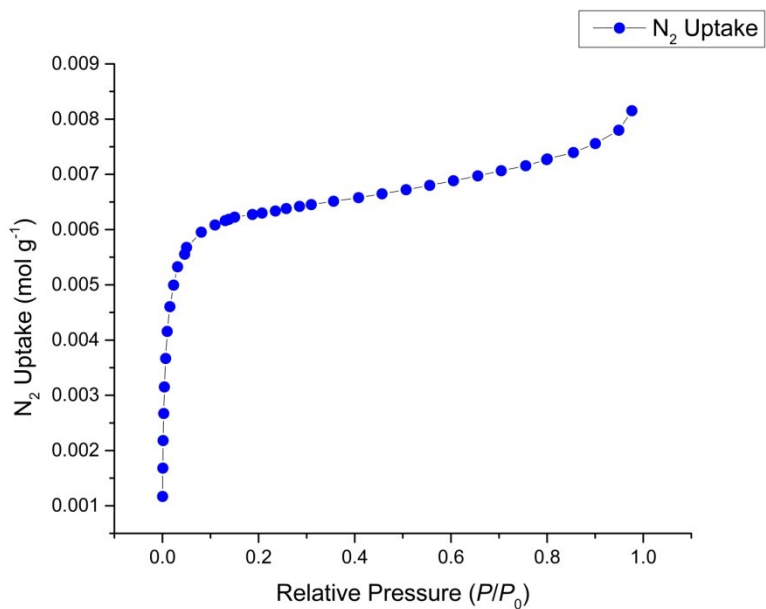
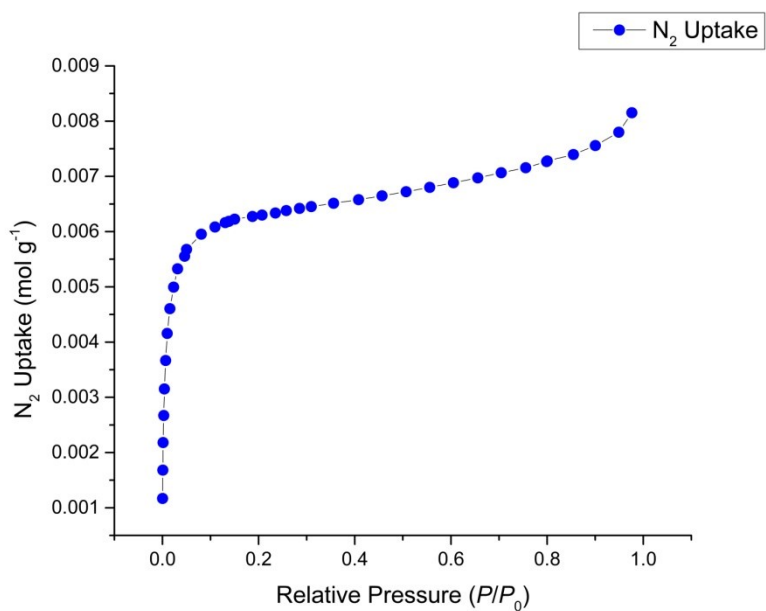**Fig. S6.** N_2 adsorption isotherm at 77 K of CAU-10 after 50 SO_2 adsorption/desorption cycles.

Fig. S7. N_2 adsorption isotherm at 77 K of CAU-10 after H_2O/SO_2 exposure.

Heat of Adsorption of SO$_2$. Additional 303 and 308 K SO$_2$ adsorption isotherms were measured to estimate the heat of adsorption, using the Clausius-Clapeyron equation (each isotherm was fitted to a Dual Site Langmuir-Freundlich isotherm, Fig. S9). A virial-type equation was used to fit the adsorption isotherms at low surface coverage, to estimate the heat of adsorption at zero coverage (Fig. S8).

The heat of adsorption starts goes from -42 to -35 kJ mol^{-1} (Fig. S10), the heat of adsorption at zero coverage was estimated in -42.8 kJ mol^{-1}.
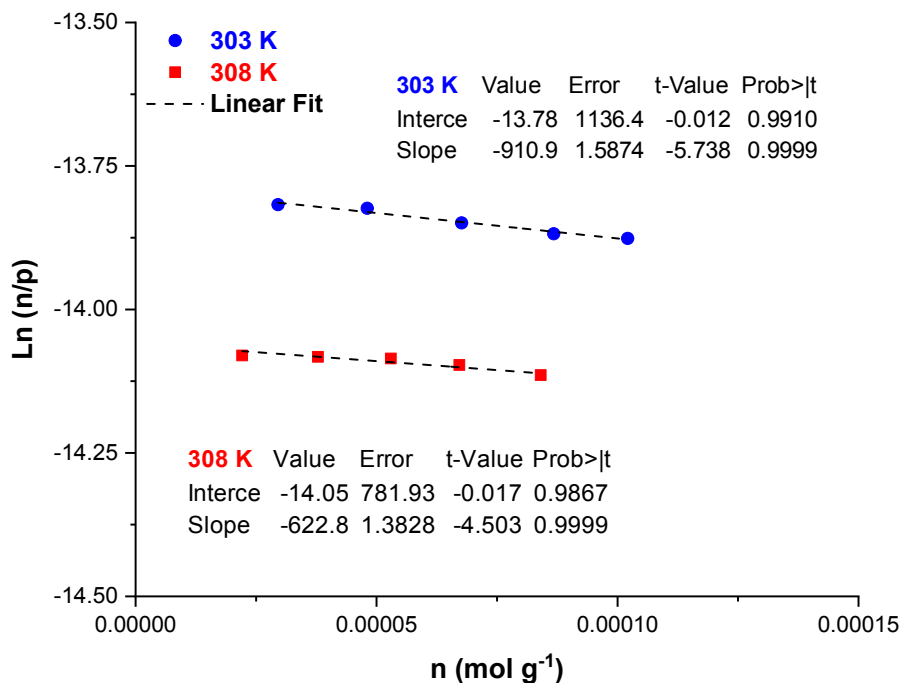

Fig. S8. Virial fit plot for the SO$_2$ adsorption at low surface coverage in CAU-10 at 303 and 308 K.
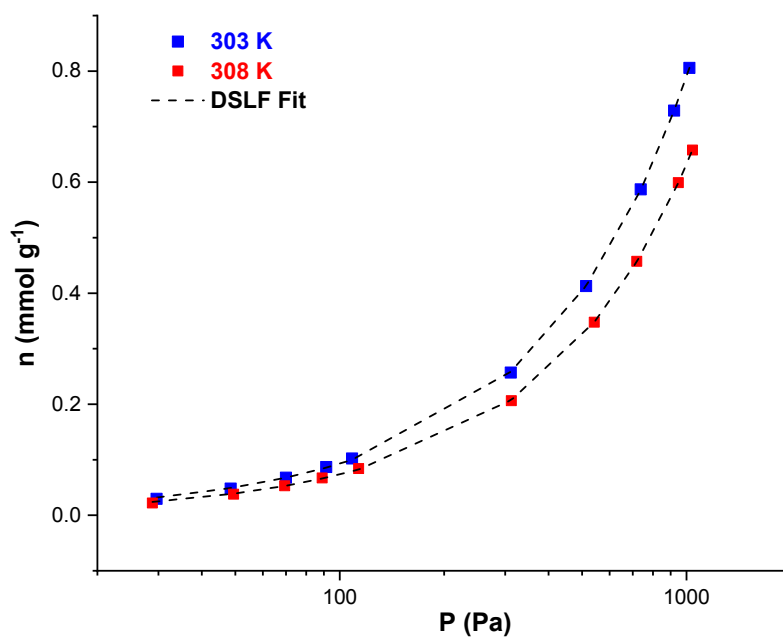
Fig. S9. CAU-10 SO$_2$ isotherms at 303 and 308 K with the corresponding Dual Site Langmuir Freundlich fits.
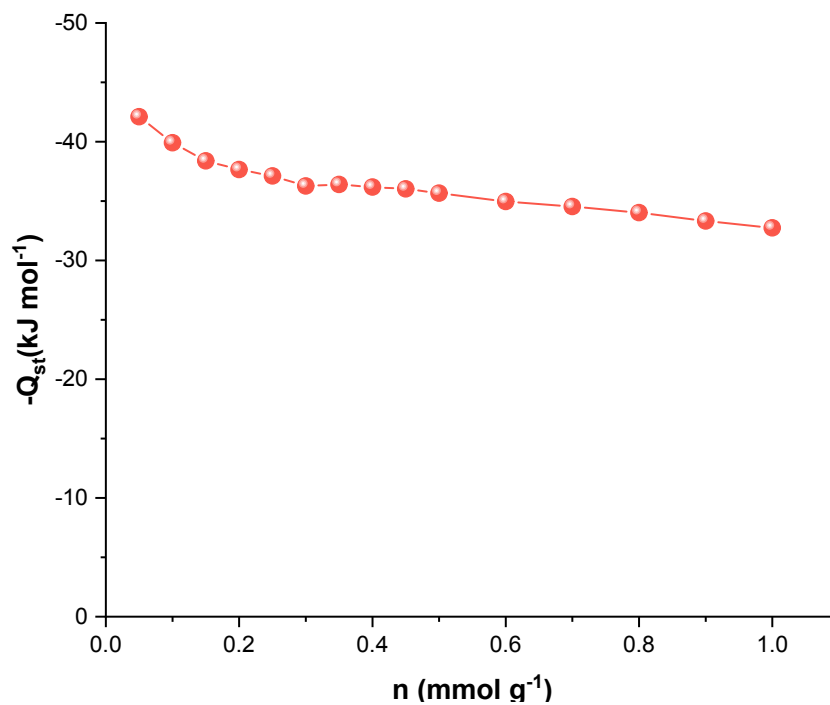
Fig. S10. CAU-10 SO$_2$ heat of adsorption as a function of the surface coverage.

Powder X-ray diffraction Experiments

X-rar powder diffraction (PXRD) were measured on a Ultima IV Rigaku X-ray diffractometer using CuKα₁ radiation (λ=1.5406 Å; monochromator: Ni) at 40 kV, 40 Ma, in a range 2-theta of 5-40° with step of 0.01°.

Fig. S11. CAU-10 PXRD pattern after SO_2 adsorption experiments (λ = 1.5406 Å).

Fig. S12. CAU-10 PXRD pattern after 50 SO_2 adsorption-desorption experiments (λ = 1.5406 Å).

Wet SO₂ Experiments

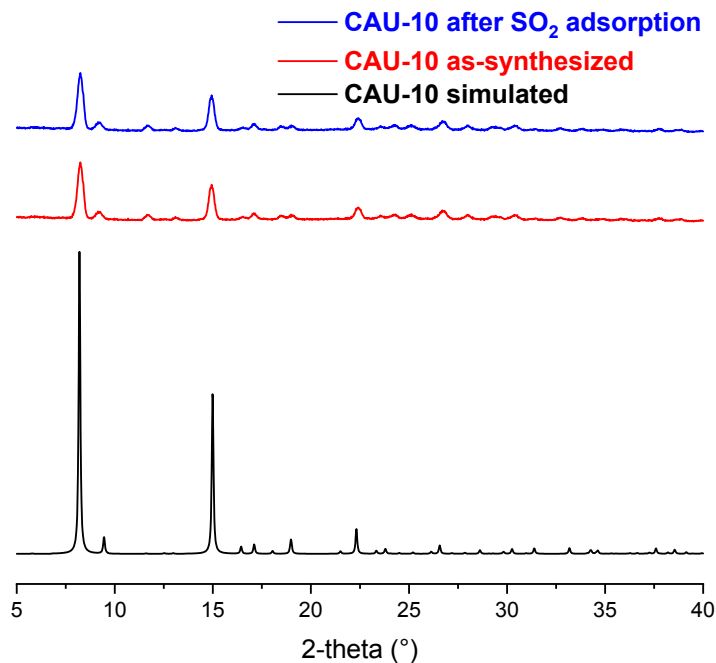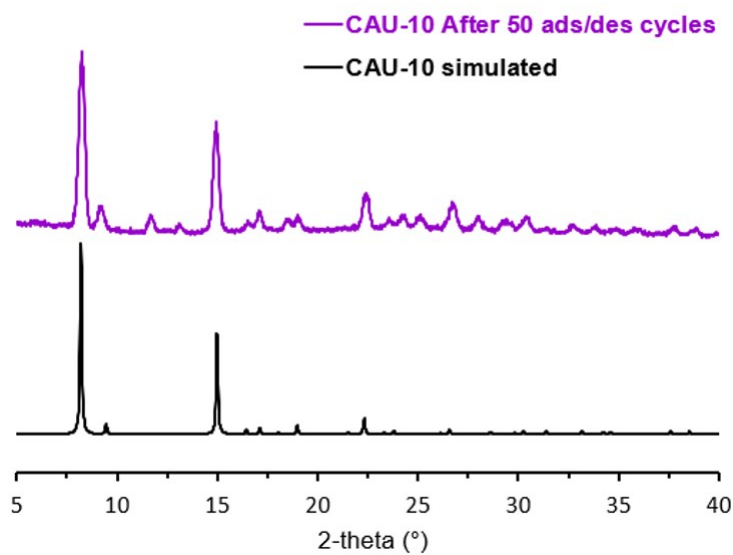The system adapted from previously reported.[2] The system contains two principal parts: SO_2 gas generator (A) dropping funnel with H_2SO_4 conc. [1] connected to a Schlenk flask with Na_2SO_3 (s) under stirring [2]; and the saturation chamber (B), constructed from a round flask with distilled water [3], connected to a sintered glass filter adapter [4] and to a vacuum line [5]. The activated sample is placed on the glass filter adapter.
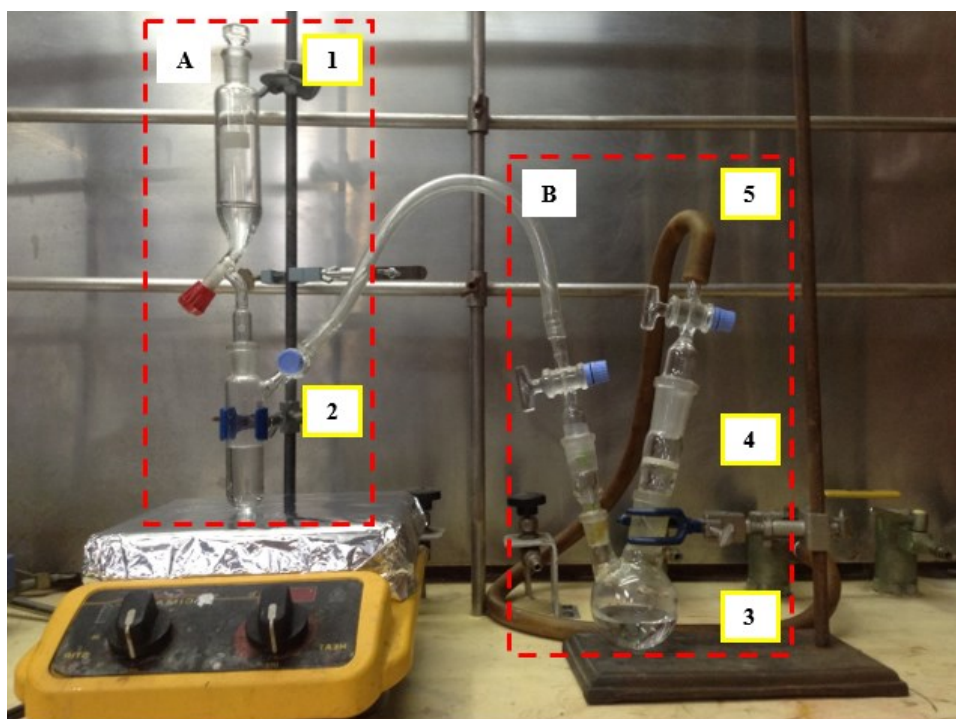
Fig. S13. Homemade system for wet SO_2 adsorption experiments.

Table S1. SO_2 adsorption capacity of some related MOFs.

Material	Formula	SO₂ uptake [mmol g⁻¹]	Temperature [K]	Ref.
CAU-10	[Al(OH)*m*-BDC]	4.7	298	This work
MFM-300(Al)	[Al₂(OH)₂BPTC]	7.1	298	3
MIL-160	[Al(OH)FDC]	7.2	293	4
MFM-300(In)	[In₂(OH)₂BPTC]	8.28	298	5
Mg-MOF-74	[Mg₂(DOBDC)]	8.6	298	6
MFM-300(Sc)	[Sc₂(OH)₂BPTC]	9.4	298	7
Ni(bdc)(ted)₀.₅		9.97	298	6
MFM-202a	[Me₂NH₂]₁.₇₅[In(BPTPC]	10.2	298	8
NH₂-MIL-125(Ti)	[Ti₈O₈(OH)₄(NH₂-BDC)₆]	10.8	293	4
Zn₂(L1)₂(bipy), L1= dibenzo-diazepine-dicarboxylate)		10.9	293	9
MFM-601	[Zn₆O₄(OH)₈(H₂O)₄(PBPTB)₂]	12.3	298	10
MOF-177	[Zn₄O(BTB)₂]	25.7	293	4

Monte Carlo Simulations

The initial atomic coordinates for CAU-10 were taken from a previous study reported by Fröhlich *et al.*[11]
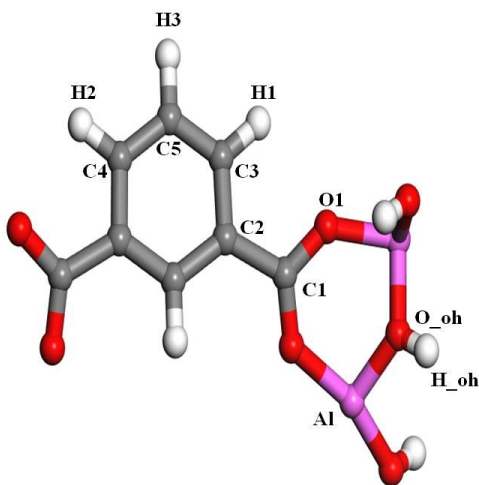
Fig. S14. Labels of the atoms for the organic and inorganic parts of CAU-10.

Table S2. Isoteric enthalpy of adsorption of SO_2 in CAU-10 from CADSS program at 298.15 K.

Pressure (bar)	Enthalpy of adsorption (kJ/mol)
0.0001	-41.7812086
0.001	-43.7641559
0.002	-44.7738584
0.003	-45.3799919
0.004	-46.2190604
0.005	-46.7147826
0.006	-46.9099277
0.007	-47.7508579
0.008	-47.3422089
0.009	-47.1959548
0.01	-47.8645893
0.02	-48.5260883
0.03	-48.3820698
0.04	-48.6767395
0.05	-49.848494
0.06	-49.3488876
0.07	-49.5715068

0.08	-48.0113747
0.09	-49.4224945
0.1	-49.871624
0.2	-47.4811952
0.3	-48.4996723
0.4	-51.6893642
0.5	-47.4834417
0.6	-48.6146033
0.7	-49.1351341
0.8	-46.7567565
0.9	-48.4476415
1	-46.1289213

In the visualization to the planes of horizontal aromatic rings **C5** along c axis (Fig. S15A) and ac plane (Fig. S15B), the planes are slightly pointing to the centre of the pore; this position forms an angle of 39.4° between them (~10° less that vertical aromatic rings), allows to C5 interact easier with incoming SO_2 molecules. The main interaction is $CH_3\cdots O$ (distance 3.99 Å, angle 29.19° C-H-O) or/and $CH_3\cdots S$ (distance 4.42 Å, angle 70.90° C-H-S).
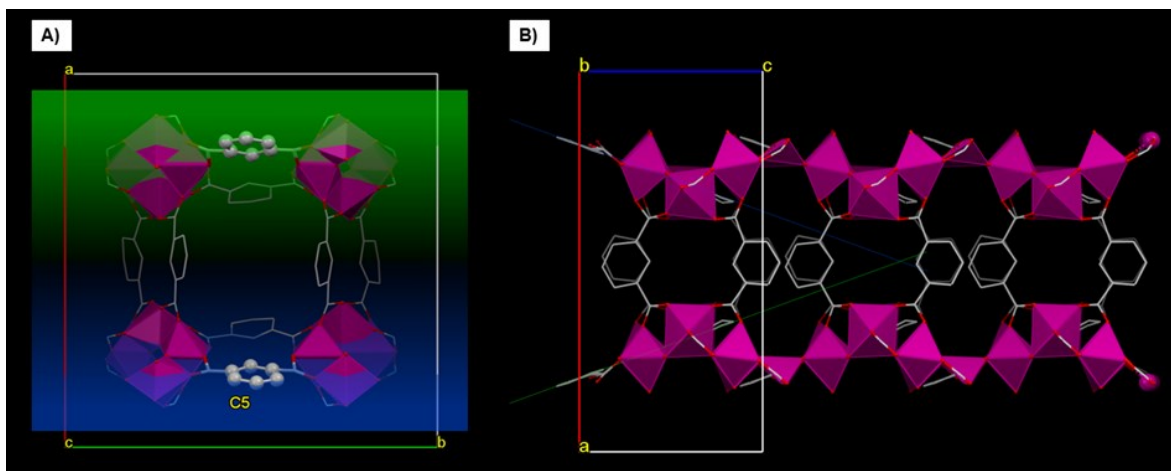

Fig. S15. View of CAU-10 pore: A) Along c axis, blue and green C5-plane; B) View of the pore through ac plane, C5-planes are slightly pointing in the centre of the pore forming an angle of 39.4°.

References

1. V. B. López-Cervantes, E. Sánchez-González, T. Jurado-Vázquez, A. Tejeda-Cruz, E. GonzálezZamora, I.A. Ibarra, CO_2 adsorption under humid conditions: Self-regulated water content in CAU-10, *Polyhedron.* 2018, **155**, 163–169. doi:10.1016/j.poly.2018.08.043.

2. S. V. Mileghem and W. M. De Borggraeve, *Org. Process Res. Dev.* 2017, **21**, 5, 785-787. doi.org/10.1021/acs.oprd.7b00083.

3. S. Yang, J. Sun, A. J. Ramirez-Cuesta, S. K. Callear, W. I. F. David, D. P. Anderson, R. Newby, A. J. Blake, J. E. Parker, C. C. Tang, M. Schröder, Selectivity and direct visualization of carbon dioxide and sulfur dioxide in a decorated porous host, *Nat. Chem.* 2012, **4**, 887–894. doi:10.1038/nchem.1457.

4. P. Brandt, A. Nuhnen, M. Lange, J. Möllmer, O. Weingart, C. Janiak, Metal–Organic Frameworks with Potential Application for SO_2 Separation and Flue Gas Desulfurization, *ACS Appl. Mater. Interfaces.* 2019, **11**, 17350-17358. doi:10.1021/acsami.9b00029.

5. M. Savage, Y. Cheng, T.L. Easun, J.E. Eyley, S.P. Argent, M.R. Warren, W. Lewis, C. Murray, C. C. Tang, M.D. Frogley, G. Cinque, J. Sun, S. Rudić, R.T. Murden, M. J. Benham, A. N. Fitch, A. J. Blake, A. J. Ramirez-Cuesta, S. Yang, M. Schröder, Selective Adsorption of Sulfur Dioxide in a Robust Metal-Organic Framework Material, *Adv. Mater.* 2016, **28**, 8705–8711. doi:10.1002/adma.201602338.

6. K. Tan, P. Canepa, Q. Gong, J. Liu, D. H. Johnson, A. Dyevoich, P. K. Thallapally, T. Thonhauser, J. Li, Y. J. Chabal, Mechanism of Preferential Adsorption of SO_2 into Two Microporous Paddle Wheel Frameworks $M(bdc)(ted)_{0.5}$, *Chem. Mater.* 2013, **25**, 4653–4662. doi:10.1021/cm401270b.

7. J. A. Zárate, E. Sánchez-González, D. R. Williams, E. González-Zamora, V. Martis, A. Martínez, J. Balmaseda, G. Maurin, I. A. Ibarra, High and energy-efficient reversible SO_2 uptake by a robust Sc(III)-based MOF, *J. Mater. Chem. A.* 2019, **7**, 15580-15584. doi:10.1039/C9TA02585E.

8. S. Yang, L. Liu, J. Sun, K. M. Thomas, A. J. Davies, M. W. George, A. J. Blake, A. H. Hill, A. N. Fitch, C. C. Tang, M. Schröder, Irreversible Network Transformation in a Dynamic Porous Host Catalyzed by Sulfur Dioxide, *J. Am. Chem. Soc.* 2013, **135**, 4954–4957. doi:10.1021/ja401061m.

9. S. Glomb, D. Woschko, G. Makhloufi, C. Janiak, Metal–Organic Frameworks with Internal UreaFunctionalized Dicarboxylate Linkers for SO_2 and NH_3 Adsorption, *ACS Appl. Mater. Interfaces.* 2017, **9**, 37419–37434. doi:10.1021/acsami.7b10884.

10. J.H. Carter, X. Han, F.Y. Moreau, I. da Silva, A. Nevin, H.G.W. Godfrey, C.C. Tang, S. Yang, M. Schröder, Exceptional Adsorption and Binding of Sulfur Dioxide in a Robust Zirconium-Based Metal–Organic Framework, *J. Am. Chem. Soc.* 2018, **140**, 15564–15567. doi:10.1021/jacs.8b08433.

11. Dominik Fröhlich, Evangelia Pantatosaki, Panagiotis D. Kolokathis, Karen Markey, Helge Reinsch, Max Baumgartner, Monique A. van der Veen, Dirk E. De Vos, Norbert Stock, George K. Papadopoulos, Stefan K. Henninger and Christoph Janiak, *J. Mater. Chem. A,* 2016,**4**, 11859